



Archived at the Flinders Academic Commons:

<http://dspace.flinders.edu.au/dspace/>

'This is the peer reviewed version of the following article:

Willmes, M., Bataille, C. P., James, H. F., Moffat, I.,
McMorrow, L., Kinsley, L., ... Grün, R. (2018). Mapping of
bioavailable strontium isotope ratios in France for
archaeological provenance studies. *Applied Geochemistry*,
90, 75–86. [https://doi.org/10.1016/
j.apgeochem.2017.12.025](https://doi.org/10.1016/j.apgeochem.2017.12.025)

which has been published in final form at

<http://dx.doi.org/10.1016/j.apgeochem.2017.12.025>

© 2017 Elsevier. This manuscript version is made
available under the CC-BY-NC-ND 4.0 license:

<http://creativecommons.org/licenses/by-nc-nd/4.0/>

Accepted Manuscript



Mapping of bioavailable strontium isotope ratios in France for archaeological provenance studies

Malte Willmes, Clement P. Bataille, Hannah F. James, Ian Moffat, Linda McMorrow, Leslie Kinsley, Richard A. Armstrong, Stephen Eggins, Rainer Grün

PII: S0883-2927(17)30413-4

DOI: [10.1016/j.apgeochem.2017.12.025](https://doi.org/10.1016/j.apgeochem.2017.12.025)

Reference: AG 4020

To appear in: *Applied Geochemistry*

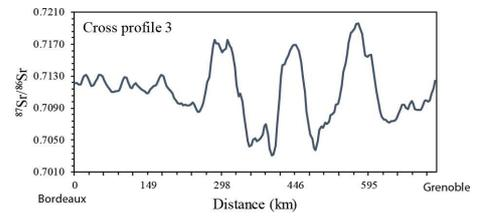
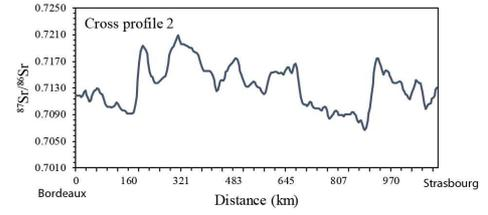
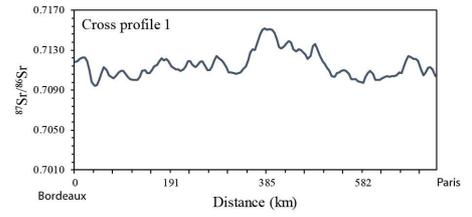
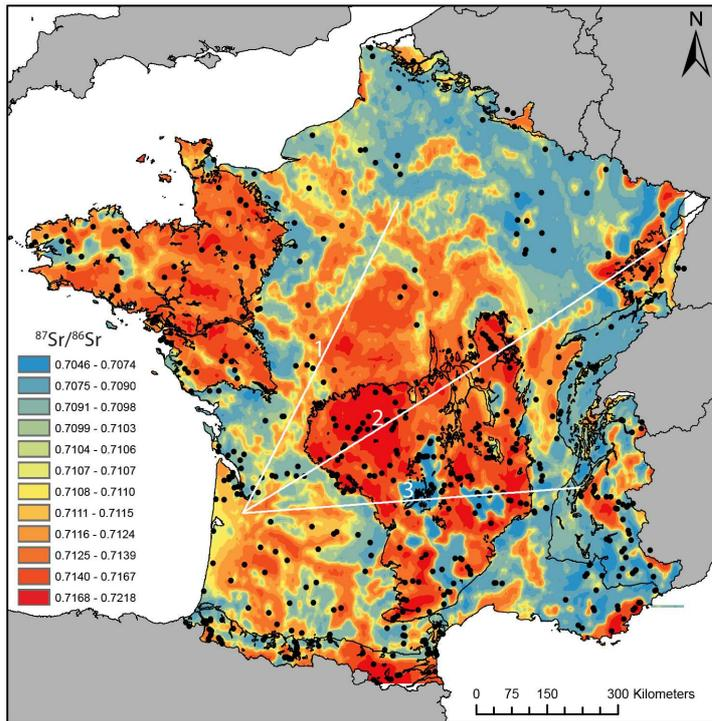
Received Date: 13 September 2017

Revised Date: 22 December 2017

Accepted Date: 27 December 2017

Please cite this article as: Willmes, M., Bataille, C.P., James, H.F., Moffat, I., McMorrow, L., Kinsley, L., Armstrong, R.A., Eggins, S., Grün, R., Mapping of bioavailable strontium isotope ratios in France for archaeological provenance studies, *Applied Geochemistry* (2018), doi: [10.1016/j.apgeochem.2017.12.025](https://doi.org/10.1016/j.apgeochem.2017.12.025).

This is a PDF file of an unedited manuscript that has been accepted for publication. As a service to our customers we are providing this early version of the manuscript. The manuscript will undergo copyediting, typesetting, and review of the resulting proof before it is published in its final form. Please note that during the production process errors may be discovered which could affect the content, and all legal disclaimers that apply to the journal pertain.



1 **Mapping of bioavailable strontium isotope ratios in France for archaeological**
2 **provenance studies**

3

4 Malte Willmes^{ab}, Clement P. Bataille^c, Hannah F. James^a, Ian Moffat^{ad}, Linda McMorrow^a, Leslie
5 Kinsley^a, Richard A. Armstrong^a, Stephen Eggins^a, Rainer Grün^{ae}

6

7 ^aResearch School of Earth Sciences, The Australian National University, Bldg. 142 Mills Rd,
8 Canberra 2602, ACT, Australia

9 ^bNow at the Department of Wildlife, Fish, and Conservation Biology, 1088 Academic Surge, One
10 Shields Avenue, University of California Davis, 95616 Davis, CA, USA

11 ^cDepartment of Earth and Environmental Sciences, University of Ottawa, Ottawa, K1N 6N5 Canada

12 ^dDepartment of Archaeology, Flinders University, Bedford Park 5042, Adelaide, SA, Australia

13 ^eAustralian Research Centre for Human Evolution, Environmental Futures Research Institute, Griffith
14 University, 170 Kessels Road, Nathan, Queensland 4111, Australia

15

16

17 Corresponding author: Malte Willmes, malte.willmes@googlemail.com

18

19 **Highlights**

- 20 • $^{87}\text{Sr}/^{86}\text{Sr}$ ratios provide a robust framework for archaeological provenance studies in France
- 21 • 5 isotope groups were identified using cluster analysis
- 22 • Kriging using the clusters as covariates produced accurate $^{87}\text{Sr}/^{86}\text{Sr}$ predictions
- 23 • This method provides a geologically and sample density informed estimate of spatial
24 uncertainty

25

ACCEPTED MANUSCRIPT

26 *Abstract*

27 Strontium isotope ratios ($^{87}\text{Sr}/^{86}\text{Sr}$) of archaeological samples (teeth and bones) can be used to track
28 mobility and migration across geologically distinct landscapes. However, traditional interpolation
29 algorithms and classification approaches used to generate Sr isoscapes are often limited in predicting
30 multiscale $^{87}\text{Sr}/^{86}\text{Sr}$ patterning. Here we investigate the suitability of plant samples and soil leachates
31 from the IRHUM database (www.irhumdatabase.com) to create a bioavailable $^{87}\text{Sr}/^{86}\text{Sr}$ map using a
32 novel geostatistical framework. First, we generated an $^{87}\text{Sr}/^{86}\text{Sr}$ map by classifying $^{87}\text{Sr}/^{86}\text{Sr}$ values into
33 five geologically-representative isotope groups using cluster analysis. The isotope groups were then
34 used as a covariate in kriging to integrate prior geological knowledge of Sr cycling with the
35 information contained in the bioavailable dataset and enhance $^{87}\text{Sr}/^{86}\text{Sr}$ predictions. Our approach
36 couples the strengths of classification and geostatistical methods to generate more accurate $^{87}\text{Sr}/^{86}\text{Sr}$
37 predictions (Root Mean Squared Error = 0.0029) with an estimate of spatial uncertainty based on
38 lithology and sample density. This bioavailable Sr isoscape is applicable for provenance studies in
39 France, and the method is transferable to other areas with high sampling density. While our method is
40 a step-forward in generating accurate $^{87}\text{Sr}/^{86}\text{Sr}$ isoscapes, the remaining uncertainty also demonstrates
41 that fine-modelling of $^{87}\text{Sr}/^{86}\text{Sr}$ variability is challenging and requires more than geological maps for
42 accurately predicting $^{87}\text{Sr}/^{86}\text{Sr}$ variations across the landscape. Future efforts should focus on
43 increasing sampling density and developing predictive models to further quantify and predict the
44 processes that lead to $^{87}\text{Sr}/^{86}\text{Sr}$ variability.

45 **Keywords:** Strontium isotopes; Tracing; Provenance; Plants; Soil leachates; Migration; Mobility

46

47 **1. Introduction**

48 Reconstructing past mobility patterns and land-use are crucial parts of understanding prehistoric
49 societies, but it is complicated by the fact that the archaeological evidence becomes scarcer with time.
50 The application of stable isotopes in archaeological research has revolutionised palaeomobility studies
51 by providing independent data, which can be used to evaluate models of migration, trade, and cultural
52 change. Strontium isotope ratios ($^{87}\text{Sr}/^{86}\text{Sr}$) have proven themselves to be a powerful tracer of
53 provenance and mobility in a wide range of fields such as archaeology, ecology, food and forensic
54 sciences (Beard and Johnson, 2000; Bentley, 2006; Hobbs et al., 2005; Kelly et al., 2005; Slovak and
55 Paytan, 2012; Voerkelius et al., 2010; West et al., 2010).

56 The underlying principle is that $^{87}\text{Sr}/^{86}\text{Sr}$ ratios vary between different geologic regions as a function
57 of bedrock age and composition (Faure and Mensing 2005). Strontium is released by weathering of
58 bedrock into the soils, ground and surface waters, from which it becomes available for uptake by
59 plants and enters the food cycle (Bentley, 2006; Capo et al., 1998). Through their diet strontium is
60 taken up by animals and humans and substitutes for calcium in biological apatite (bones, teeth), where
61 it serves no metabolic function. Consequently, the $^{87}\text{Sr}/^{86}\text{Sr}$ ratio measured in a bone or tooth, will
62 reflect the average of dietary Sr, that was consumed while the skeletal tissue was forming (Beard and
63 Johnson, 2000; Bentley, 2006). Thus, $^{87}\text{Sr}/^{86}\text{Sr}$ ratios can be used to reconstruct changes in food
64 sources and by extension residence area by comparing the values obtained from a skeletal tissue with a
65 baseline map of strontium isotopic variation across a region (e.g., Bentley, 2006; Slovak and Paytan,
66 2011).

67 A complicating factor is that the $^{87}\text{Sr}/^{86}\text{Sr}$ ratio of Sr available to biological organisms (termed
68 bioavailable strontium) can differ from the bulk $^{87}\text{Sr}/^{86}\text{Sr}$ isotopic composition of the bedrock, due to
69 the preferential weathering of certain minerals with different $^{87}\text{Sr}/^{86}\text{Sr}$ ratios (Sillen et al., 1998). In
70 addition, the isotopic composition of the bioavailable strontium can be influenced by atmospheric
71 deposition (precipitation, sea spray, dust), the presence of exogenous surface deposits (loess, glacial
72 till, cover sands, peat), mixing processes between different strontium reservoirs, and anthropogenic
73 influences such as fertilizer application and air pollution (Bentley, 2006; Evans et al., 2010; Frei and
74 Frei, 2013; Maurer et al., 2012; Price et al., 2002; Slovak and Paytan, 2012; Widga et al., 2017). These
75 processes vary between different areas and may introduce significant shifts in the bioavailable $^{87}\text{Sr}/^{86}\text{Sr}$
76 ratio compared to the expected values based on bedrock geology.

77 Consequently, a variety of samples types have been used to create baseline bioavailable $^{87}\text{Sr}/^{86}\text{Sr}$ maps
78 including rock leachates, soil leachates, plant samples, surface and ground water samples,
79 archaeological and modern fauna or human remains (Bentley, 2006; Evans et al., 2009; Evans and
80 Tatham, 2004; Maurer et al., 2012; Price et al., 2002; Slovak and Paytan, 2012). The best suited
81 sample material for archaeological provenance studies are archaeological samples with the same food
82 source range as the archaeological samples in question, such as well-preserved teeth with a known
83 local origin (e.g. rodents). However, these are not available for large-scale (e.g. country wide) studies

84 and thus substitute sample materials are needed. Despite this, no consensus currently exists in the
85 literature as to what type of sample material is best suited to determine the overall spatial variability of
86 bioavailable $^{87}\text{Sr}/^{86}\text{Sr}$ isotope ratios for a country wide study.

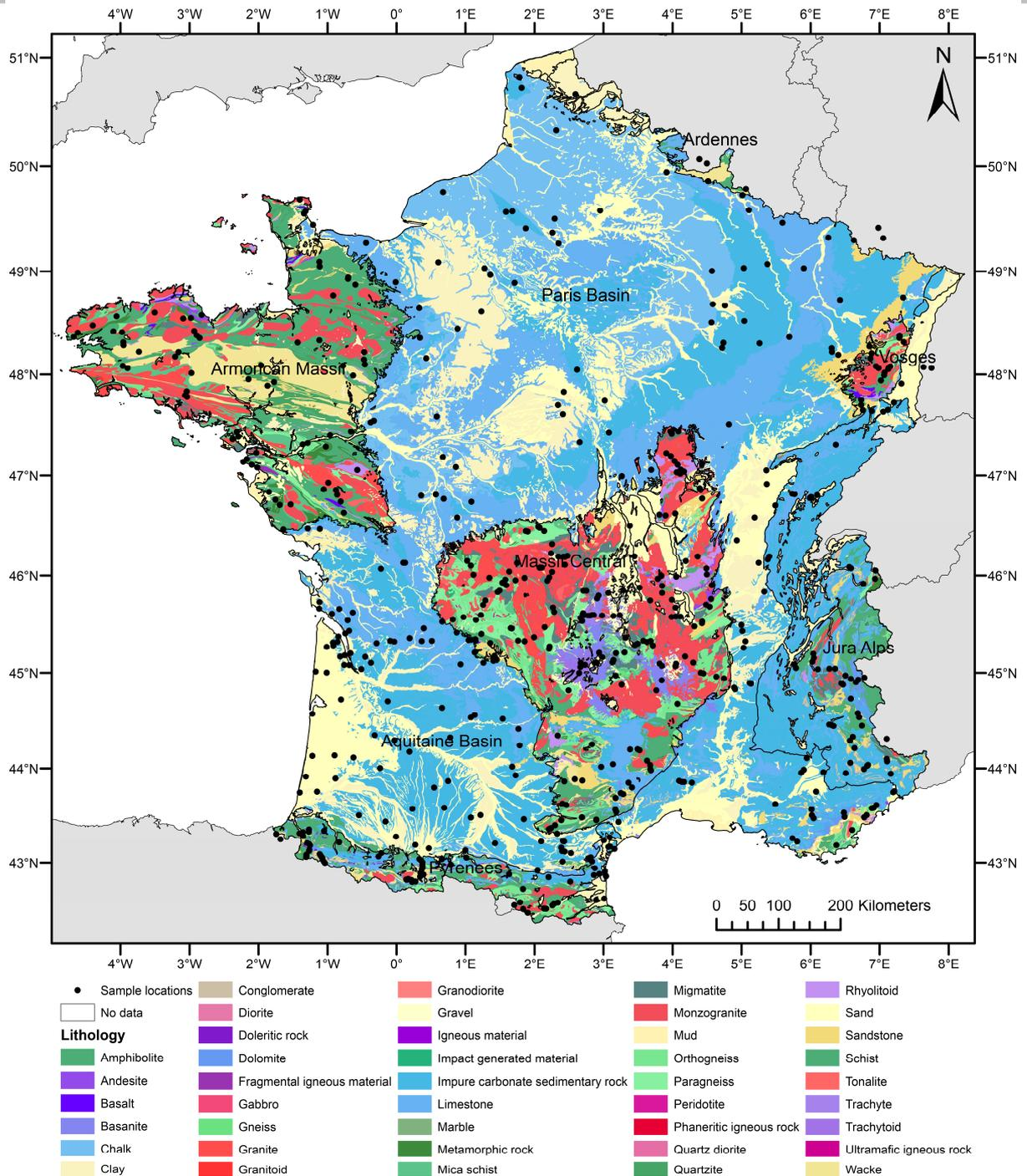
87 Terrestrial baseline $^{87}\text{Sr}/^{86}\text{Sr}$ ratio maps using different sample types and modelling methods have been
88 produced for a number of regions at varying scales and spatial resolutions, for example for Europe
89 (Voerkelius et al., 2010), Britain (Evans et al., 2010, 2009), Denmark (Frei and Frei, 2011, 2013),
90 Netherlands (Kootker et al., 2016), Israel (Hartman and Richards, 2014), the contiguous USA (Bataille
91 and Bowen, 2012; Beard and Johnson, 2000), Alaska (Bataille et al., 2014; Brennan et al., 2014), the
92 Caribbean region (Bataille et al., 2012; Laffoon et al., 2012), Mesoamerica (Hodell et al., 2004),
93 Puerto Rico (Pestle et al., 2013), South Africa (Copeland et al., 2016; Sillen et al., 1998), and South
94 Korea (Song et al., 2014). In addition, archaeological provenance studies on smaller spatial scales
95 have been carried out in many areas around archaeological sites producing local baseline maps
96 (Bentley, 2006; Price et al., 2004, 2002; Slovak and Paytan, 2012).

97 Currently, only limited baseline $^{87}\text{Sr}/^{86}\text{Sr}$ data exists for France, hindering the use of $^{87}\text{Sr}/^{86}\text{Sr}$ ratios for
98 investigating the provenance of samples from the vast archaeological record in France. The aim of this
99 study is to build on the previously published dataset of $^{87}\text{Sr}/^{86}\text{Sr}$ ratios of plants and soil leachates
100 (Willmes et al., 2014) to produce a bioavailable $^{87}\text{Sr}/^{86}\text{Sr}$ baseline map for archaeological provenance
101 studies for continental France.

102 **2. Data and methods**

103 **2.1 Sample selection**

104 The IRHUM (Isotopic Reconstruction of Human Migration) database is a web platform for sharing
105 and mapping $^{87}\text{Sr}/^{86}\text{Sr}$ ratios from environmental samples (Willmes et al., 2014). For continental
106 France, it presently contains 843 sample locations from which plant samples and top soil leachates
107 have been analysed for $^{87}\text{Sr}/^{86}\text{Sr}$ ratios (Pangaea data repository doi:10.1594/PANGAEA.819142,
108 www.irhumdatabase.com). The analytical methods are described in detail in Willmes et al. (2014). In
109 brief, plant samples are considered to represent a direct measure of bioavailable Sr and were ashed and
110 completely dissolved. Soil samples were subjected to a ammonium nitrate (NH_4NO_3) leaching process
111 to extract the bioavailable part of the bulk strontium (Capo et al., 1998; Gryschko et al., 2005; Hall et
112 al., 1998; Meers et al., 2007; Prohaska et al., 2005; Rao et al., 2008; Sillen et al., 1998). Sr
113 concentrations and $^{87}\text{Sr}/^{86}\text{Sr}$ ratios were measured at the Research School of Earth Sciences (RSES).
114 We selected 610 sample locations from the dataset, which cover all major geologic units and
115 lithologies of France (Figure 1). This subset of the IRHUM dataset excludes sample locations that are
116 situated on geologic units that are not characteristic for their geographic area, such as minor geologic
117 outcrops ($<10 \text{ km}^2$), river terraces, as well as sample sites that are likely to represent modern
118 anthropogenic activity, such as agricultural fields and managed forest areas.



119

120 **Figure 1:** Surface geologic map of France (BRGM) with sample sites from the IRHUM dataset marked as black
 121 dots.

122 2.2 Spatial and statistical methods

123 The strontium isotope data from the IRHUM database were spatially joined with the geologic map of
 124 France (Chantraine et al., 2005) and the surface geologic map of France (BRGM) using ESRI
 125 ArcGIS™. The definitions of the lithological units are taken from the OneGeology-Europe project
 126 (<http://www.onegeology-europe.org>). The data were then screened to check that the described
 127 lithology from the IRHUM dataset matches the lithology from the geologic maps. In case of

128 discrepancies the lithology was matched to the closest corresponding geological unit. Finally, we
129 removed minor lithological units from the data (e.g. impact generated rocks, mud, amphibols,
130 quartzites) and simplified and merged the lithological information to achieve uniform descriptions of
131 units across France. For non-parametric statistical analysis Microsoft Excel and R (R Core Team,
132 2017) were used. For the box and whisker plot the top and bottom of the box are defined as the third
133 and first quartiles. The interquartile range (IQR) is calculated by subtracting the first quartile from the
134 third. The second quartile, which is the median, is shown as a black line. The whiskers are defined as
135 $Q1-1.5*IQR$ for the lower whisker and $Q3+1.5*IQR$ for the upper whisker. Cluster analysis was
136 conducted using R with the cluster (Maechler et al., 2015), fpc (Hennig, 2015), and clValid (Brock et
137 al., 2008) packages.

138

139 2.3 Kriging methods

140 Kriging is a geostatistical interpolation method, which depends on statistical models of spatial
141 autocorrelation (Goovaerts, 1998; Krige, 1951; Saby et al., 2006). Briefly, the trends in spatial
142 autocorrelation between pairs of points from a given dataset are modelled by fitting a curve or
143 “variogram model”. This variogram model is then used as a basis to interpolate the target variable
144 away from the points. Several versions of kriging have been developed but in this study, we focus on
145 ordinary kriging and kriging with external drift. Ordinary kriging is the most commonly used, it
146 predicts a value at any given location by using the local mean and a variogram model of the spatial
147 autocorrelation. Kriging with external drift is similar but instead of using the local mean, it estimates a
148 trend based on an auxiliary predictor, and solves simultaneously for second order effects. In this study,
149 we use the map of isotopes packages derived from the cluster analysis as the primary auxiliary
150 variable in the kriging with external drift approach. All kriging was carried out separately for soil and
151 plant samples using the geostatistical toolbox in ArcGIS (ESRI). Both soil and plant data are evaluated
152 separately and in addition a combined soil and plant layer is generated by averaging the two original
153 geostatistical layers (predictions and estimated errors) using the raster toolbox in ArcGIS (ESRI).

154

155 3. Results and Discussion

156 3.1 Comparison of strontium isotope ratios in plant and soil samples

157 In theory, both soil leachates, which represent the bioavailable Sr of the soil, and plant samples, which
158 are a direct measure of the bioavailable Sr, should result in similar $^{87}\text{Sr}/^{86}\text{Sr}$ ratios at a given sample
159 location (Blum et al., 2000; Hodell et al., 2004). 499 sample locations in this study contain data for
160 both plant samples and soil leachates and thus can be used to investigate potential differences between
161 these sample types. We define the difference between plant samples and soil leachates as $\Delta_{\text{PS}} =$
162 $(^{87}\text{Sr}/^{86}\text{Sr}_{\text{plant}} - ^{87}\text{Sr}/^{86}\text{Sr}_{\text{soil leachate}})$. Overall, we find a strong positive correlation between the plant and

163 soil $^{87}\text{Sr}/^{86}\text{Sr}$ ratios ($R=0.94$). The average Δ_{PS} value, calculated from absolute values, is
164 0.0008 ± 0.0012 (σ , $n=499$), median is 0.0002. However, some sample sites show a significantly higher
165 offset between plant and soil samples. The largest Δ_{PS} is -0.0085 , which encompasses a large part of
166 the entire $^{87}\text{Sr}/^{86}\text{Sr}$ ratio variation of France at a single sample location. Sites with large Δ_{PS} values
167 show that soil and plant samples collected in very close spatial context can still represent vastly
168 different strontium isotope reservoirs (Figure 2). This has been observed in previous studies (Blum et
169 al., 2000; Evans et al., 2010; Evans and Tatham, 2004; Hodell et al., 2004; Maurer et al., 2012), and
170 can result from a multitude of different processes.

171 The primary driver for $^{87}\text{Sr}/^{86}\text{Sr}$ isotopic variation across a landscape is the underlying geology and
172 thus differences in Δ_{PS} may also be related to difference between lithologies. Soils and plants in
173 geologically complex areas may form on geochemically highly mixed substrates, caused by the
174 weathering of different rock types and different minerals within the same rock (e.g., Sillen et al.,
175 1998). Thus, lithological complex units (e.g., gravels, granites, orthogneisses) are expected to show
176 higher average Δ_{PS} values than geochemical homogenous lithological units (e.g., limestones). For
177 example, we find high Δ_{PS} values for gravel units that could reflect their heterogeneous composition
178 consisting of rock fragments with potentially vastly different $^{87}\text{Sr}/^{86}\text{Sr}$ ratios placed next to each other.
179 However, in contrast to this hypothesis, the average Δ_{PS} values of limestones and granites are similar
180 (Table 1). The majority of soils are not only the product of *in situ* weathering but a composite of
181 different processes and different strontium sources. Overall, we find high average Δ_{PS} values both in
182 heterogeneous as well as in homogenous geologic substrates, indicating that the underlying geology is
183 not the only driver for the observed difference between soil and plant samples.

184 Differences in $^{87}\text{Sr}/^{86}\text{Sr}$ values between top soil and plant samples are influenced by a plant's root
185 depth, which may allow the sampling of soil horizons with differing $^{87}\text{Sr}/^{86}\text{Sr}$ values and the plant's
186 susceptibility to atmospheric deposition of strontium (Drouet et al., 2007; Maurer et al., 2012; Poszwa
187 et al., 2004, 2002). In this study, we concentrated on top soil samples and shallow rooted plants
188 (grasses, shrubs). We dissolved the entire plant rather than specific tissues to mitigate this potential
189 source of variability. Grasses should more closely reflect the $^{87}\text{Sr}/^{86}\text{Sr}$ ratio of the topsoil than other
190 plant species with deeper roots. However, we observe high Δ_{PS} values for all plant sample types
191 including grass samples (Figure 3). There is no significant difference in average Δ_{PS} values for grass
192 samples (mean=0.00082, median=0.00041, $n=380$) compared to tree roots (mean=0.00086,
193 median=0.00042, $n=35$) and other plant sample types (mean=0.00083, median=0.00038, $n=84$). The
194 exception being moss samples that show higher average Δ_{PS} values (mean=0.00107, median=0.0046,
195 $n=35$). Finally, both soil and plant samples have a similar variance of 0.00002, indicating that the
196 variability did not decrease as strontium was moved from the soil into the plant.

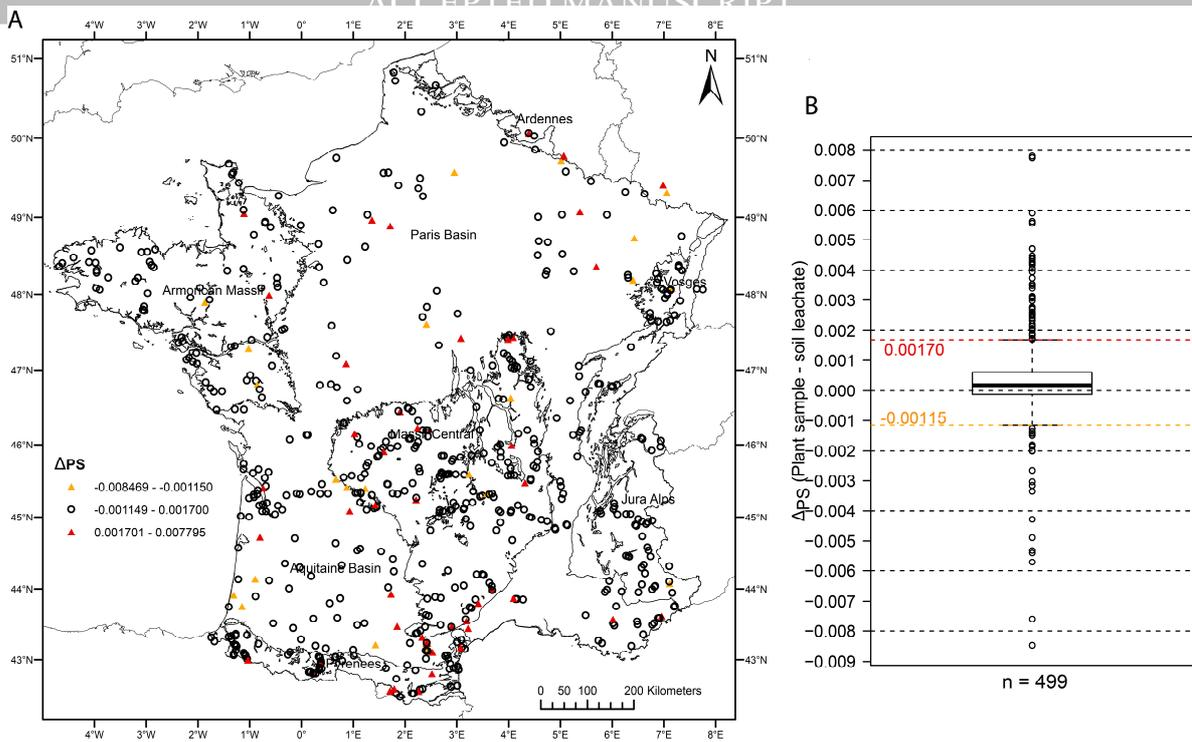
197 External input of strontium, such as precipitation, sea spray, and dust, can potentially create difference
198 between sample materials. As a first order observation, we find no direct spatial correlation between

199 the occurrence of Δ_{PS} values and precipitation and land use. However, these processes could not be
200 investigated in detail because we are lacking the data to constrain the $^{87}\text{Sr}/^{86}\text{Sr}$ ratios of these sources.

201 Finally, on the scale of France, it is likely that at any given sample location a combination of the
202 discussed processes is at work. Identification of the driver of Δ_{PS} values is confounded by the complex
203 interplay between weathering of lithology, soil genesis, plant processes, and external strontium inputs
204 that vary both in absolute strontium concentrations as well as isotope ratios, spatially and with time.
205 Based solely on the strontium isotope ratios it is not possible to untangle these processes and
206 quantification of external strontium inputs was beyond the scope of this work. We intend to revisit a
207 range of sites to conduct detailed sampling to investigate the differences between plant samples and
208 soil leachates. Concerning the aim of this study, which is to create a robust baseline map, we
209 incorporated the observed local variability but excluded outlier sites that are not representative of their
210 lithological unit and geographic area. This approach does not favour a specific sample material, taking
211 into account that there are likely multiple processes at work that create the variations in $^{87}\text{Sr}/^{86}\text{Sr}$ ratios
212 observed at specific sites. We classify outlier Δ_{PS} values based on the boxplot (Figure 2) as any value
213 above $Q3 + 1.5 \times IQR$ or below $Q1 - 1.5 \times IQR$ (+0.00170 and -0.00115, respectively). In total, 70
214 sample locations (~14%) have Δ_{PS} values outside of this range (Table 1). Removing these sample
215 locations results in a dataset with an average Δ_{PS} value of 0.0004 ± 0.0004 (1σ , $n=429$) and improves
216 the correlation between plant and soil samples ($R= 0.99$). The risk in removing these sites is that it
217 could potentially lead to an underestimation of the strontium isotopic variability for certain lithological
218 units. We tested this by comparing the strontium isotope range for each lithological unit from the
219 complete and the outlier removed dataset. No significant differences are observed, indicating that
220 removing the outliers did not affect the overall strontium isotopic variability of the different
221 lithological units. The exceptions are the gravel and chalk units, which show significantly narrower
222 strontium isotope ranges after outlier removal. However, these lithologies are represented only by a
223 small number of samples (gravel $n=5$, chalk $n=8$). The results for these two units should thus be
224 treated with caution and specifically the gravel samples cannot be considered to represent the full
225 strontium isotopic range of these units for France.

226 **Table 1:** Summary statistics of the Δ_{PS} values for the different lithological units. Δ_{PS} values are calculated as absolute values, ignoring the direction of the offset between the
 227 sample types.

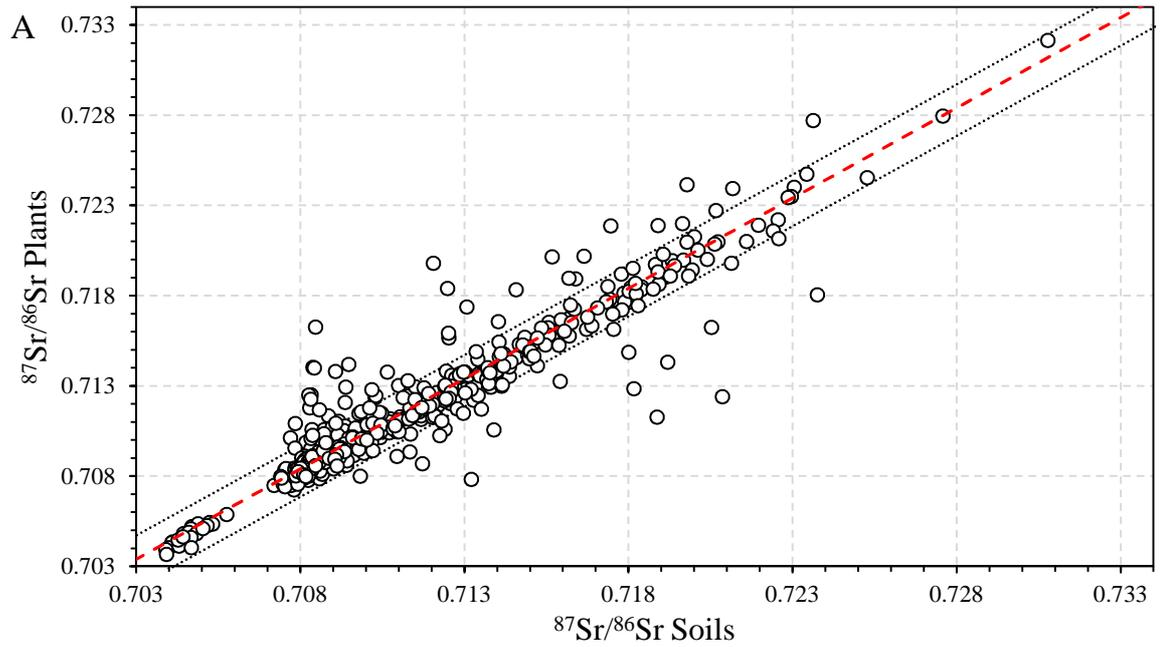
Lithologies	Δ_{PS} (plant sample - soil leachate)			Outlier				
	Min	Max	Average	Sample pairs [n]	1σ	Sample pairs [n]	%	Outlier removed average Δ_{PS}
Volcanics (Basanites, Tephrites, Pyroclastica, Trachytes)	0.00001	0.00065	0.00022	22	0.00017	0	0	0.00022
Chalk	0.00006	0.00563	0.00147	6	0.00213	2	33	0.00034
Dolomite	0.00013	0.00047	0.00028	4	0.00014	0	0	0.00028
Limestone	0.00001	0.00557	0.00066	67	0.00107	6	9	0.00036
Impure carbonate sedimentary rock	0.00001	0.00471	0.00079	95	0.00094	14	15	0.00047
Clay	0.00002	0.00760	0.00096	26	0.00160	5	19	0.00036
Sand	0.00000	0.00774	0.00082	52	0.00132	8	15	0.00041
Gravel	0.00023	0.00531	0.00207	5	0.00217	2	40	0.00023
Conglomerate	0.00006	0.00572	0.00128	15	0.00176	4	27	0.00036
Sandstone	0.00007	0.00429	0.00094	20	0.00111	4	20	0.00047
Wacke	0.00010	0.00066	0.00031	3	0.00031	0	0	0.00031
Granite	0.00001	0.00847	0.00067	64	0.00119	4	6	0.00043
Paragneiss	0.00001	0.00145	0.00048	15	0.00037	0	0	0.00048
Orthogneiss	0.00001	0.00437	0.00096	19	0.00100	3	16	0.00073
Migmatite	0.00005	0.00590	0.00091	15	0.00150	2	13	0.00041
Schist	0.00002	0.00780	0.00113	55	0.00155	12	22	0.00045
Mica schist	0.00006	0.00090	0.00038	5	0.00039	0	0	0.00038
Rhyolitoid	0.00015	0.00375	0.00130	11	0.00133	3	27	0.00055
All lithologies	0.00000	0.00847	0.00082	499	0.00123	70	14	0.00043



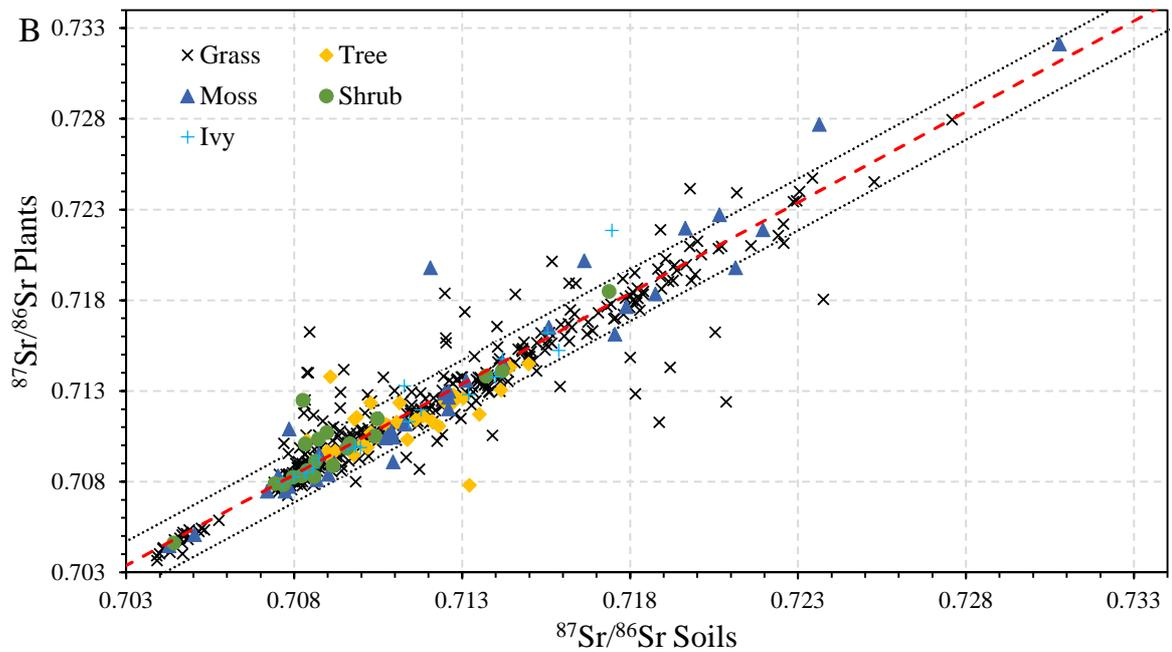
229

230 **Figure 2:** A: Geographic distribution of Δ_{PS} values in France and B: Boxplot of the Δ_{PS} values. Outliers are
 231 defined by the whiskers, as any value higher than 0.00170 and lower than -0.00115.

232



234



235

236 **Figure 3:** $^{87}\text{Sr}/^{86}\text{Sr}$ ratios of plants plotted against soil leachate values from the same site. A: Plot including all
 237 sample pairs, a linear fit is shown in red. Grey lines are the top and bottom whisker from the boxplot of Δ_{PS}
 238 values (Figure 2), and any data point outside of the grey lines is identified as an outlier. B, same data plotted as
 239 in A, classified based on plant type.

240

241 3.2 Strontium isotope groups

242 The dataset presented here consists of 540 sample locations, with a total of 968 individual samples,
243 after outlier removal. The bioavailable $^{87}\text{Sr}/^{86}\text{Sr}$ ratios for each lithological unit are shown in Figure 4,
244 Table 2, and significant overlap in $^{87}\text{Sr}/^{86}\text{Sr}$ ratios exists between different lithological units.

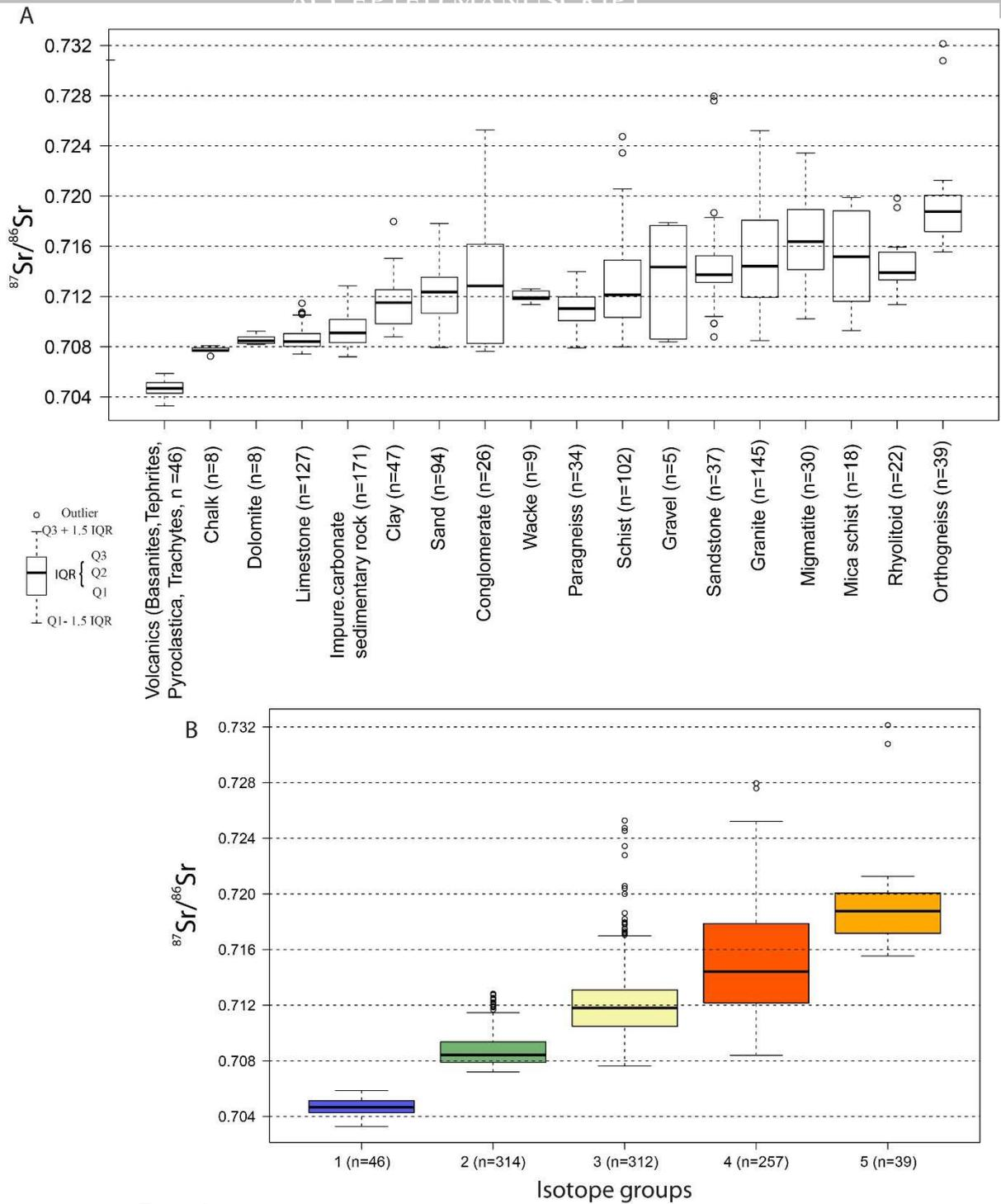
245 We performed cluster analysis to identify groups of lithological units with minimized internal variance
246 and maximum difference between groups in $^{87}\text{Sr}/^{86}\text{Sr}$ ratios. Several different clustering techniques
247 (hierarchal, k-means, pam) were tested and k-means clustering set to 5 clusters was found to produce
248 the highest optimized values, as determined by cluster validation (optimal Silhouette and Dunn
249 values). Bedrock age is often used as a classifier to group $^{87}\text{Sr}/^{86}\text{Sr}$ ratios as older and more rubidium
250 rich rocks have higher $^{87}\text{Sr}/^{86}\text{Sr}$ ratios, but in this dataset lithology rather than age was found to be a
251 better cluster variable. We grouped the lithological units and their strontium isotope ranges into 5
252 isotope groups. The contribution of each lithological unit to its isotope group was weighted by the
253 relative area of that lithological unit.

254 We defined the following isotope groups:

- 255 • Isotope group 1 (0.7033-0.7059) includes the volcanic units (basanites, tephrites, trachytoids)
256 predominantly found within the Massif Central.
- 257 • Isotope group 2 (0.7072-0.7115) is comprised of the carbonaceous sediments (chalk, dolomite,
258 limestone, impure carbonate sedimentary rocks) and is the dominant lithology in the Aquitaine
259 Basin, Paris Basin and Alpine Foreland.
- 260 • Isotope group 3 (0.7076-0.7170) comprises the clay, sand, conglomerate wacke, paragneiss, schist
261 units. The clastic sediments are found within the basins along rivers intercutting the units of
262 isotope group 2 as well as along the Atlantic coastline. Paragneiss and schist units are found in the
263 mountainous regions with large outcrops in the Armorican Massif, Massif Central, and in the
264 Pyrenees.
- 265 • Isotope group 4 (0.7084-0.7252) is composed of the gravel, sandstone, granite, migmatite, mica
266 schist, and rhyolitoid units. These units are found dominantly in the mountainous regions of
267 France.
- 268 • Isotope group 5 (0.7155-0.7213) includes the orthogneiss units found in the Massif Central and
269 Pyrenees.

270 The isotope group map (Figure 5) is a simplified representation of the bioavailable $^{87}\text{Sr}/^{86}\text{Sr}$ ranges of
271 the lithological units and first strontium isotope baseline map for France. Since it is based on the
272 surface geologic map it is accurate in displaying the sharp geologic boundaries and their
273 corresponding changes in bioavailable $^{87}\text{Sr}/^{86}\text{Sr}$ ratios. Limitations of the map are that because

274 lithology was used as classification it does not allow us to investigate isotopic variation within single
275 lithological units. The large strontium isotope ranges and significant overlaps (Figure 6) are a direct
276 result of using the broad lithological units as classifiers for the isotope groups. For example, granites
277 are represented as one unit, but different types of granites can have vastly different initial Rb
278 concentrations and resulting $^{87}\text{Sr}/^{86}\text{Sr}$ ratios. A similar effect can be observed in the clastic sediments,
279 which vary significantly in their $^{87}\text{Sr}/^{86}\text{Sr}$ ratios depending on their source region (e.g., between
280 mountainous areas and the basins) but are here grouped together causing an increase in their internal
281 variability. Consequently, the main limitation of this map is related to the high variability in $^{87}\text{Sr}/^{86}\text{Sr}$
282 ratios observed for many lithological units. This map can thus be used to identify broad geographic
283 patterns of residence change, but may not resolve smaller scale mobility and land-use changes within
284 similar $^{87}\text{Sr}/^{86}\text{Sr}$ isotopic regions. For example, isotope group 1 is constrained to a small area in the
285 Massif Central and thus a sample with a corresponding isotope value could be placed into a tight
286 geographic constrain, while samples with isotope values similar to isotope group 2 could correspond
287 to many areas in the Paris and Aquitaine Basin. This reflects both the high variability found in isotope
288 group 2 as well as the fact that distant geographic locations may exhibit closely similar $^{87}\text{Sr}/^{86}\text{Sr}$ ratios
289 based on their similar underlying geology.

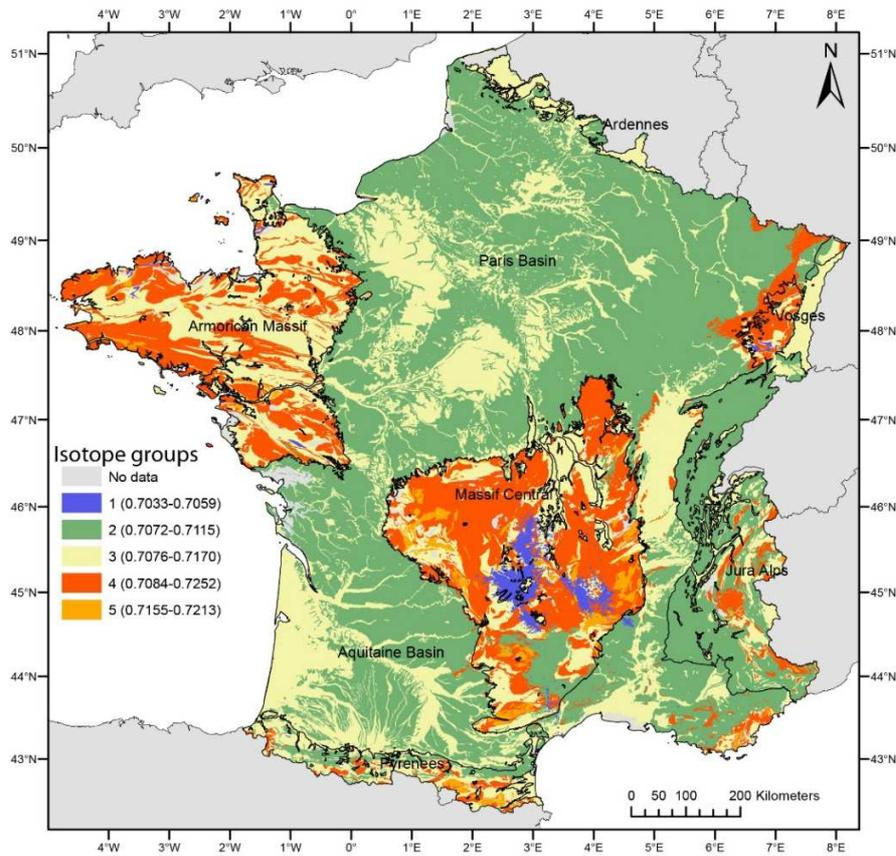


290

291 **Figure 4:** Box and whisker plot of the bioavailable $^{87}\text{Sr}/^{86}\text{Sr}$ range, A for each lithology and B for the 5 isotope
 292 groups (n=number of samples). The isotope groups combine lithologies to minimize the internal variance and
 293 maximize the difference between groups.

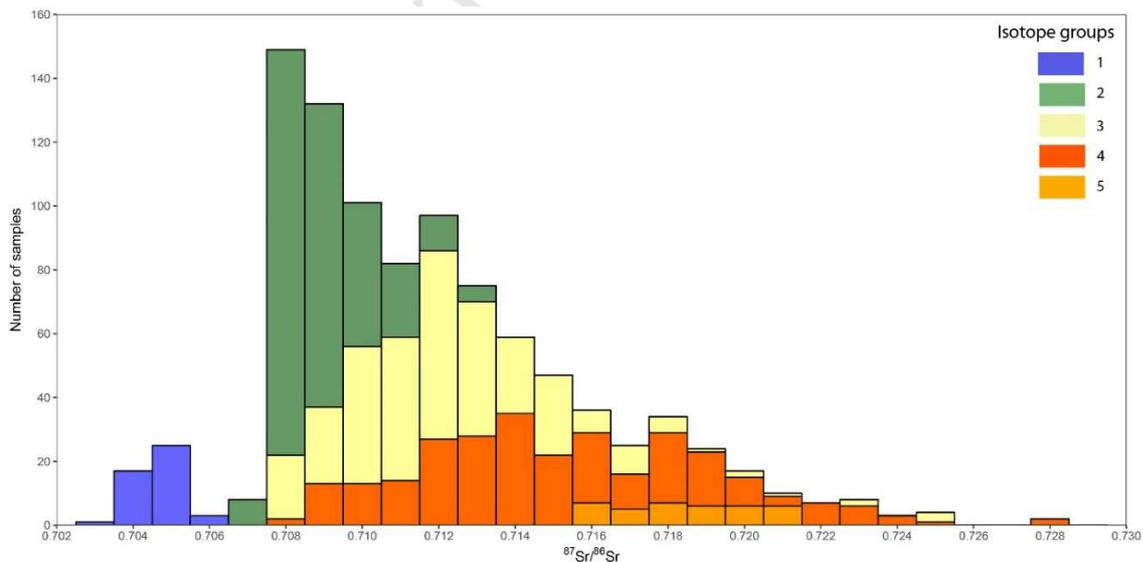
294 **Table 2:** Summary statistics for the bioavailable $^{87}\text{Sr}/^{86}\text{Sr}$ range for each lithology and the isotope groups.

Lithologies	Isotope Group	Bioavailable $^{87}\text{Sr}/^{86}\text{Sr}$					Q3+1.5* IQR	n	Area [km ²]
		Q1-1.5 *IQR	Q1	Q2	Q3				
Volcanics	1	0.70328	0.70428	0.70468	0.70514	0.70587	46	12693	
Chalk	2	0.70764	0.70765	0.70770	0.70790	0.70808	8	100291	
Dolomite	2	0.70818	0.70825	0.70846	0.70877	0.70923	8	5772	
Limestone	2	0.70741	0.70802	0.70842	0.70904	0.71052	127	172254	
Imp. carb. sedi. rock	2	0.70720	0.70832	0.70910	0.71017	0.71284	171	252846	
Clay	3	0.70877	0.70983	0.71152	0.71253	0.71504	47	114622	
Sand	3	0.70794	0.71067	0.71236	0.71354	0.71781	94	159230	
Conglomerate	3	0.70763	0.70825	0.71284	0.71617	0.72528	26	2562	
Wacke	3	0.71136	0.71177	0.71191	0.71244	0.71261	9	25385	
Paragneiss	3	0.70790	0.71007	0.71104	0.71196	0.71399	34	20603	
Schist	3	0.70799	0.71035	0.71214	0.71489	0.72057	102	75615	
Gravel	4	0.70839	0.70862	0.71434	0.71766	0.71788	5	1800	
Sandstone	4	0.71041	0.71312	0.71374	0.71525	0.71829	37	27438	
Granite	4	0.70849	0.71193	0.71441	0.71808	0.72521	145	100313	
Migmatite	4	0.71022	0.71414	0.71638	0.71893	0.72343	30	16332	
Mica schist	4	0.70928	0.71161	0.71518	0.71883	0.71989	18	14434	
Rhyolitoid	4	0.71135	0.71332	0.71390	0.71552	0.71593	22	9635	
Orthogneiss	5	0.71555	0.71717	0.71876	0.72007	0.72126	39	18940	
Isotope Group	1	0.70328	0.70428	0.70468	0.70514	0.70587	46	12693	
	2	0.70720	0.70790	0.70842	0.70937	0.71147	314	531163	
	3	0.70763	0.71048	0.71180	0.71311	0.71699	312	398017	
	4	0.70839	0.71216	0.71441	0.71786	0.72521	257	169952	
	5	0.71555	0.71717	0.71876	0.72007	0.72126	39	18940	



295

296 **Figure 5:** Map of the surface geologic lithologies of France, coloured by their classification into the 5
 297 isotope groups.



298

299 **Figure 6:** Histogram of $^{87}\text{Sr}/^{86}\text{Sr}$ ratios from soil and plant samples, coloured by isotope group.

300 3.3 Kriging

301 Significant overlap in $^{87}\text{Sr}/^{86}\text{Sr}$ ratios exists between different lithological units, showing that the
302 strontium isotope ratios form a continuum rather than specific readily distinguishable groups. To take this
303 into account and to incorporate the variability in strontium isotope ratios within the larger geological units
304 (used previously as classifiers) we performed kriging to interpolate the $^{87}\text{Sr}/^{86}\text{Sr}$ ratios between sample
305 locations (Table 3). Kriging generates a smooth continuous surface and allows us to investigate more
306 subtle changes in $^{87}\text{Sr}/^{86}\text{Sr}$ ratios within geologic units. We compared ordinary kriging and kriging with
307 external drift using the geological cluster map as a covariate for both soil and plant samples (Figure 7).
308 Ordinary kriging resulted in a root-mean-square error (RMSE) of 0.0032 for soils and 0.0031 for plant
309 samples. Kriging with external drift gave an improved RMSE with 0.0029 for both sample types. In
310 addition, the use of the isotope groups as covariate in the kriging with external produces a strontium
311 isoscape that more closely reflects the expected pattern of $^{87}\text{Sr}/^{86}\text{Sr}$ variations (Bataille and Bowen, 2012).
312 Discrete $^{87}\text{Sr}/^{86}\text{Sr}$ variations following geological clusters dominate at large spatial scale whereas more
313 continuous intra-unit variations reflect local geochemical heterogeneity. This pattern of $^{87}\text{Sr}/^{86}\text{Sr}$
314 variations is in contrast with the continuous $^{87}\text{Sr}/^{86}\text{Sr}$ variations produced by ordinary kriging which can
315 only map $^{87}\text{Sr}/^{86}\text{Sr}$ variations as broad gradients with prediction rapidly deteriorating away from the
316 bioavailable sampling sites. The pattern also differs from the $^{87}\text{Sr}/^{86}\text{Sr}$ cluster map by accounting for the
317 intra-unit variability and by smoothing the discrete geological boundaries in the $^{87}\text{Sr}/^{86}\text{Sr}$ variability. The
318 increase in prediction conformity with the current knowledge of Sr cycling is also visible when looking at
319 individual transect of $^{87}\text{Sr}/^{86}\text{Sr}$ predictions through France. The map produced using kriging with external
320 drift shows rapid shift of $^{87}\text{Sr}/^{86}\text{Sr}$ values at geological boundaries (e.g. Massif Central vs. sedimentary
321 basins) as well as more diffuse boundaries associated with geomorphological processes (e.g. river
322 valleys). River valleys accumulate sediments from isotopically distinct parent rocks which differ from the
323 local bedrock $^{87}\text{Sr}/^{86}\text{Sr}$ values. For instance, the Loire, Garonne, or Seine rivers display higher $^{87}\text{Sr}/^{86}\text{Sr}$
324 values than the surrounding rock units because they are transporting sediments from older radiogenic rock
325 units upstream.

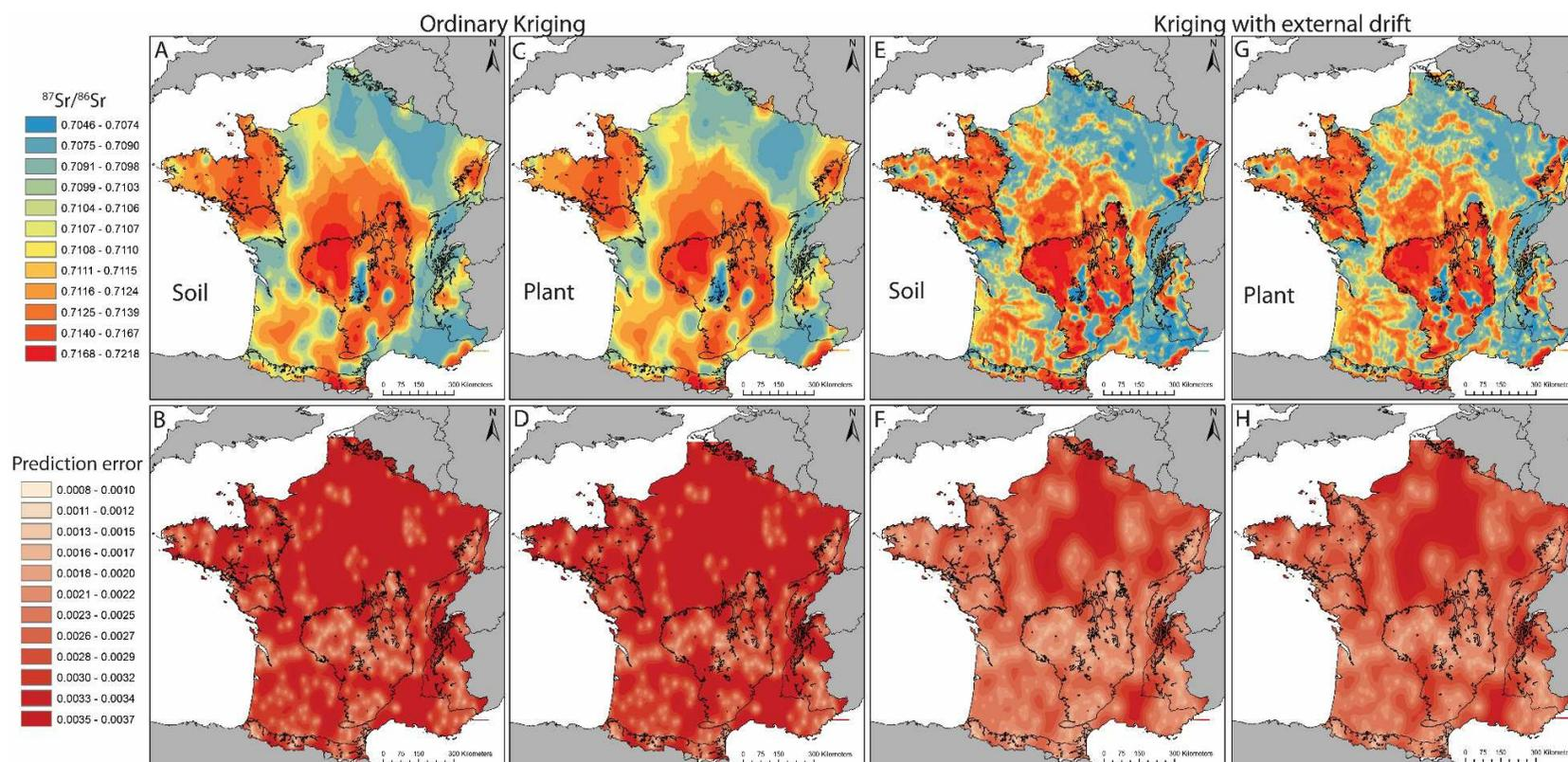
326 Advantageously, kriging also provides estimates of spatial uncertainty which is critical to integrate
327 $^{87}\text{Sr}/^{86}\text{Sr}$ models in quantitative framework of geographic assignment (Wunder, 2012). The RMSE value
328 of 0.0029 (12% of the whole $^{87}\text{Sr}/^{86}\text{Sr}$ dataset range) for kriging with external drift for the combined soil
329 and plant dataset demonstrates that significant uncertainty remains in predicting $^{87}\text{Sr}/^{86}\text{Sr}$ variations and
330 would significantly limit quantitative geographic assignment efforts. However, when comparing the
331 spatial uncertainty map generated by ordinary kriging and kriging with external drift, the variance is
332 significantly reduced in the kriging with external drift. The ordinary kriging variance shows a bullseye

333 pattern, centred around sampling sites, that is heavily dependent on the range of the fitted variogram
 334 model with prediction becoming rapidly uncertain away from the points. Conversely, the kriging with
 335 external drift shows much lower variance away from the point as it integrates both the predictive potential
 336 of the bioavailable dataset and that of the covariate. While this spatial uncertainty is markedly reduced,
 337 the kriging variance remains high in areas with very low sampling density (e.g. Paris Basin and Rhone
 338 delta). Additional sampling coupled with improved geostatistical framework to incorporate existing
 339 geospatial covariates would further improve the accuracy and resolution of those models. As a summary,
 340 the kriging with geological clusters as external drift produces a more detailed and realistic strontium
 341 isotope map of France than either the isotope group methods or the ordinary kriging methods. Those
 342 methods are, to date, the two most commonly applied methods to map $^{87}\text{Sr}/^{86}\text{Sr}$ variations (Copeland et
 343 al., 2016; Evans et al., 2010; Hodell et al., 2004). Our method proposes to combine these previous
 344 approaches in a two-step process to reach higher predictive power.

345 Table 3: Kriging method parameters.

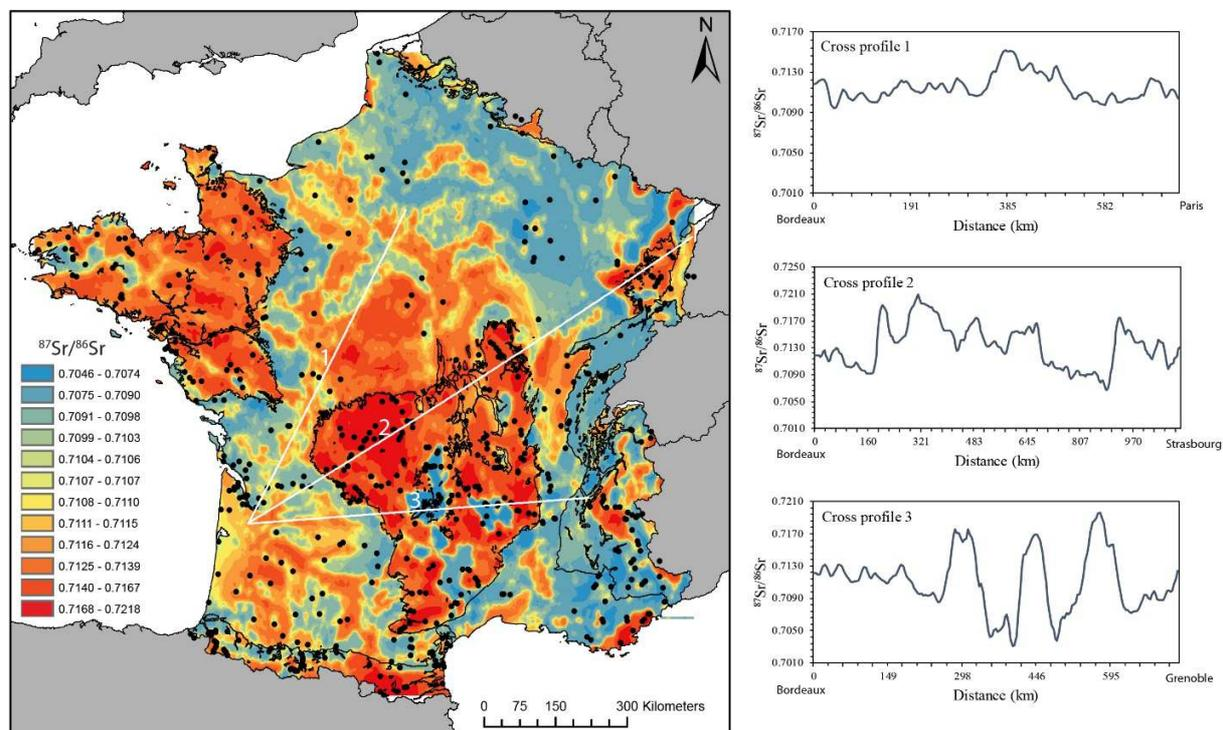
Method	Transformation	Trend removal	Variogram model	Search Neighbourhood	Sectors	RMSE
Ordinary Kriging	None	None	Exponential	Standard	4	Soils: 0.00308
				Min: 5		Plants: 0.00318
				Max: 50		
Kriging with External Drift	None	Constant	Exponential	Standard	4	Soils: 0.00290
				Min: 5		Plants: 0.00289
				Max: 50		

346



347

348 **Figure 7:** Results from Ordinary kriging for soils (A, B) and plants (C, D) and Kriging with external drift for soil (E, F) and plants (G, H). No
 349 significant differences are observed between soil and plant samples. Kriging with external drift outperforms Ordinary kriging and produces
 350 significantly lower prediction errors. High prediction errors remain in areas of low sample density.



351
 352 **Figure 8:** Strontium isoscape of France based on combined soil and plant samples with kriging with
 353 external drift. Three example cross profiles are shown (white lines), originating from Bordeaux and going
 354 to Paris (Cross profile 1), Strasbourg (Cross profile 2), and Grenoble (Cross profile 3). Black dots
 355 represent the sample locations.

356 3.4 Application to archaeological provenance studies

357 France exhibits a significant contrast in $^{87}\text{Sr}/^{86}\text{Sr}$ ratios making it a suitable area to apply strontium
 358 isotopes for archaeological provenance studies (Figure 8). The map produced in this study represents the
 359 first large scale bioavailable $^{87}\text{Sr}/^{86}\text{Sr}$ baseline for all of France and provides a powerful new tool for
 360 archaeological studies when taking the following limitations into account.

- 361 (1) The sample density is low given the large geographic area of France and only covers major
 362 geologic units. Increasing sample density will likely resolve finer scale patterns of strontium
 363 isotopic variation across the landscape. The prediction error maps (Figure 7F, H) provide a direct
 364 indication of where additional samples are needed to improve this map, mainly the northern
 365 border of the Massif Central and the Paris Basin.

- 366 (2) The large $^{87}\text{Sr}/^{86}\text{Sr}$ ranges found in many lithological units and isotope groups, and the occurrence
367 of similar lithological units with overlapping $^{87}\text{Sr}/^{86}\text{Sr}$ ranges at geographically distant areas in
368 France may limit the identification of mobility and land-use between those areas. This is
369 showcased in the three example cross profiles across France (Figure 8). Along cross profile 1
370 (Bordeaux to Paris), many geographically distant areas have similar $^{87}\text{Sr}/^{86}\text{Sr}$ ratios, which would
371 limit the identification of mobility along this vector. On the other hand, cross profile 2 (Bordeaux
372 to Strasbourg) and cross profile 3 (Bordeaux to Grenoble), cross the Massif Central and exhibit
373 many geographically distinct $^{87}\text{Sr}/^{86}\text{Sr}$ ratios, which would allow for a detailed investigation of
374 mobility across this landscape. The sequence and timing of the $^{87}\text{Sr}/^{86}\text{Sr}$ ratios can further help
375 identify mobility patterns, when it can be retrieved from the skeletal material, by for example
376 multiple teeth from a single individual or using in-situ methods to extract time resolved
377 information from a sample.
- 378 (3) The extent of the strontium baseline map is constrained to present day France, which creates
379 boundaries with no significant meaning for many archaeological provenance studies. This can be
380 overcome by including other strontium isotope baseline maps and detailed local studies into the
381 analysis. This is facilitated by founding the baseline map on the surface geologic map of Europe,
382 which uses consistent lithological identifiers across all of Europe and sharing the data on the
383 IRHUM database (Willmes et al., 2014).
- 384 (4) Another limitation of the baseline map presented here is caused by the use of modern
385 environmental samples. For example, the last ice age has significantly influenced the distribution
386 of surface deposits in many parts of Europe and this needs to be considered when applying a map
387 like this to trace human mobility and land-use in the distant past. The spatial distribution of
388 exogenous surface deposits (Scheib et al., 2014) could be used to identify problematic areas that
389 may have been significantly altered in recent geological time. In addition, climatological and
390 atmospheric conditions change and thus could have a temporally variable effect on the strontium
391 isotope ratios measured in plants and soils. Modern samples that are affected by anthropogenic
392 influences are problematic in this regard and need to be avoided for the creation of a baseline map
393 for archaeological provenance studies. Care was taken during sample selection to avoid these
394 areas using information from the GEMAS (Reimann et al., 2014) and CORINE land use dataset
395 (European Environment Agency (EEA), 2009).
- 396 (5) An additional limitation of this map is that it does not take atmospheric deposition of strontium
397 into account to delineate different isotopic regions. The atmospheric deposition of strontium from
398 precipitation, sea spray, and dust can have a significant contribution to the $^{87}\text{Sr}/^{86}\text{Sr}$ ratios of

399 plants and soils in France. Due to their spatially and temporally complex patterns it was not
400 possible to quantify their contribution to the bioavailable $^{87}\text{Sr}/^{86}\text{Sr}$ ranges for the lithological units
401 in this study. Thus, the $^{87}\text{Sr}/^{86}\text{Sr}$ ranges established in this map may not adequately reflect times
402 of greatly different climatological and atmospheric regimes in the past.

403 (6) Similarly, anthropogenic inputs of strontium are not considered in this map. Samples were
404 selected from sites that should minimize these inputs, nevertheless in a country such as France
405 anthropogenic inputs are likely and not always identifiable in the field. Artificial fertilizers and
406 soil amendments are commonly used in Europe and may contribute a significant component to
407 the Sr content in soil and plant material. Only very restricted information is available on the Sr
408 concentration and isotopic composition of artificial fertilizers. A comprehensive study of
409 fertilizers in Spain (Vitòria et al., 2004) found that there is a large variation in $^{87}\text{Sr}/^{86}\text{Sr}$ ratios for
410 different fertilizers spanning most of the geological materials on Earth. Most fertilizers showed
411 $^{87}\text{Sr}/^{86}\text{Sr}$ ratios around 0.708-0.709 thus overlapping with modern seawater compositions.
412 However, depending on their source, fertilizers can have highly variable Sr concentrations and
413 $^{87}\text{Sr}/^{86}\text{Sr}$ ratios. Other anthropogenic sources are urban and industrial wastes \sim 0.708 and
414 detergents \sim 0.709-0.710 (Vitòria et al., 2004). A case study investigating the Allanche river
415 watershed in the Massif Central found that while there was a high fertilizer input of dissolved
416 major ions, the Sr source was dominated (\sim 90%) by bedrock weathering (Négrel and Deschamps,
417 1996). Studies of stream and ground water in the mountainous areas of France such as Armorican
418 Massif and Massif Central have found variable influence of fertilizers and have related generally
419 low $^{87}\text{Sr}/^{86}\text{Sr}$ ratios to manure from livestock farming (0.7092-0.7109) and fertilizer application
420 (0.7079-0.7095) (Négrel, 1999; Négrel et al., 2004). Data from the GEMAS atlas do not show a
421 systematic and significant difference between the extractable Sr content of agricultural or grazing
422 soils (Reimann et al., 2014), indicating that fertilizer application might not be a major source of
423 Sr for soils in many areas in France.

424 We recommend using this map (Figure 8) in combination with detailed strontium isotopic studies around
425 the archaeological site in question. In this capacity, it provides a powerful tool to identify possible
426 residence and food source areas. For the application to provenance human or animal remains we can
427 make use of the fact that these animals will average their food source over a geographic area and time.
428 Thus, more extreme $^{87}\text{Sr}/^{86}\text{Sr}$ values are less likely to contribute significantly, increasing our ability to
429 identify different regions and thus allowing a more nuanced interpretation of the data. The map is also a
430 useful tool to determine where strontium isotopic tracing studies should best be applied and what kind of
431 geographic resolution can be expected.

432 4. Conclusions

433 This study presents the first bioavailable $^{87}\text{Sr}/^{86}\text{Sr}$ baseline map using a kriging with external drift
434 approach, as a tool for archaeological provenance studies in France. The resulting map combines the
435 strengths of discrete classification and geostatistical models and provides accurate $^{87}\text{Sr}/^{86}\text{Sr}$ predictions
436 with a geologically and sample density informed estimate of spatial uncertainty. While this map presents
437 a significant step forward in generating accurate $^{87}\text{Sr}/^{86}\text{Sr}$ isoscapes, the high remaining uncertainty also
438 demonstrates that fine-modelling of $^{87}\text{Sr}/^{86}\text{Sr}$ variability is challenging and requires more than geological
439 maps for accurately predicting $^{87}\text{Sr}/^{86}\text{Sr}$ variations on the surface. More in-depth studies are needed to
440 quantify the spatial and temporal variability of the input from different strontium reservoirs into soils and
441 plants which is the likely source of the observed offsets between sample types at a number of sample
442 locations. Future studies should focus on increasing sampling density, developing predictive models and
443 apply novel geostatistical frameworks to further quantify and predict the processes that lead to $^{87}\text{Sr}/^{86}\text{Sr}$
444 variability across the landscape. Finally, combining the $^{87}\text{Sr}/^{86}\text{Sr}$ isoscape map with additional isotopic
445 and elemental tracers (such as oxygen and lead) could further constrain the vector and distance of
446 mobility and facilitate more nuanced archaeological interpretations.

447

448 Acknowledgements

449 We thank Bruno Maureille, Maxime Aubert, Patrice Courtaud, Christophe Falguères, Graham Mortimer,
450 Philippe Rossi, Ceridwen Boel, Magdalena Huyskens, Eric Ward, and Nigel Craddy for their unwavering
451 support with this project. Funding was provided by ARC DP110101415 (Grün, Spriggs, Armstrong,
452 Maureille and Falguères) *Understanding the migrations of prehistoric populations through direct dating
453 and isotopic tracking of their mobility patterns*. Part of this research was supported by the Australian
454 French Association for Science & Technology through the ACT Science Fellowship program (2013) to
455 M. Willmes. The authors thank the four anonymous reviewers whose constructive and thorough critique
456 significantly improved the quality of this manuscript.

457

458 **References**

- 459 Bataille, C.P., Bowen, G.J., 2012. Mapping $87\text{Sr}/86\text{Sr}$ variations in bedrock and water for large scale
460 provenance studies. *Chem. Geol.* 304–305, 39–52. doi:10.1016/j.chemgeo.2012.01.028
- 461 Bataille, C.P., Brennan, S.R., Hartmann, J., Moosdorf, N., Wooller, M.J., Bowen, G.J., 2014. A
462 geostatistical framework for predicting variations in strontium concentrations and isotope ratios in
463 Alaskan rivers. *Chem. Geol.* 389, 1–15. doi:10.1016/j.chemgeo.2014.08.030
- 464 Bataille, C.P., Laffoon, J., Bowen, G.J., 2012. Mapping multiple source effects on the strontium isotopic
465 signatures of ecosystems from the circum-Caribbean region. *Ecosphere* 3, 1–24. doi:10.1890/ES12-
466 00155.1
- 467 Beard, B.L., Johnson, C.M., 2000. Strontium isotope composition of skeletal material can determine the
468 birth place and geographic mobility of humans and animals. *J. Forensic Sci.* 45, 1049–61.
- 469 Bentley, R.A., 2006. Strontium Isotopes from the Earth to the Archaeological Skeleton: A Review. *J.*
470 *Archaeol. Method Theory* 13, 135–187. doi:10.1007/s10816-006-9009-x
- 471 Blum, J.D., Taliaferro, E.H., Weisse, M.T., Holmes, R.T., 2000. Changes in Sr/Ca, Ba/Ca and $87\text{Sr}/86\text{Sr}$
472 ratios between trophic levels in two forest ecosystems in the northeastern U.S.A. *Biogeochemistry*
473 49, 87–101. doi:10.1023/A:1006390707989
- 474 Brennan, S.R., Fernandez, D.P., Mackey, G., Cerling, T.E., Bataille, C.P., Bowen, G.J., Wooller, M.J.,
475 2014. Strontium isotope variation and carbonate versus silicate weathering in rivers from across
476 Alaska: Implications for provenance studies. *Chem. Geol.* 389, 167–181.
477 doi:10.1016/j.chemgeo.2014.08.018
- 478 BRGM, n.d. Geology of France at 1:1million scale (6th edition) - OneGeology-Europe project - WP6.
- 479 Brock, G., Pihur, V., Datta, S., Datta, S., 2008. cIValid: An R Package for Cluster Validation. *J. Stat.*
480 *Software*, 25, 1–22.
- 481 Capo, R.C., Stewart, B.W., Chadwick, O.A., 1998. Strontium isotopes as tracers of ecosystem processes:
482 theory and methods. *Geoderma* 82, 197–225. doi:10.1016/S0016-7061(97)00102-X
- 483 Chantraine, J., Chêne, F., Nehlig, P., Rabu, D., 2005. Carte géologique de la France à 1/1 000 000 6e
484 édition révisée 2003. BRGM.
- 485 Copeland, S.R., Cawthra, H.C., Fisher, E.C., Lee-Thorp, J.A., Cowling, R.M., le Roux, P.J., Hodgkins, J.,
486 Marean, C.W., 2016. Strontium isotope investigation of ungulate movement patterns on the
487 Pleistocene Paleo-Agulhas Plain of the Greater Cape Floristic Region, South Africa. *Quat. Sci. Rev.*

- 488 141, 65–84. doi:10.1016/j.quascirev.2016.04.002
- 489 Drouet, T., Herbauts, J., Gruber, W., Demaiffe, D., 2007. Natural strontium isotope composition as a
490 tracer of weathering patterns and of exchangeable calcium sources in acid leached soils developed
491 on loess of central Belgium. *Eur. J. Soil Sci.* 58, 302–319. doi:10.1111/j.1365-2389.2006.00840.x
- 492 European Environment Agency (EEA), 2009. Corine land cover.
- 493 Evans, J.A., Montgomery, J., Wildman, G., 2009. Isotope domain mapping of $^{87}\text{Sr}/^{86}\text{Sr}$ biosphere
494 variation on the Isle of Skye, Scotland. *J. Geol. Soc. London.* 166, 617–631. doi:10.1144/0016-
495 76492008-043
- 496 Evans, J.A., Montgomery, J., Wildman, G., Boulton, N., 2010. Spatial variations in biosphere $^{87}\text{Sr}/^{86}\text{Sr}$
497 in Britain. *J. Geol. Soc. London.* 167, 1–4. doi:10.1144/0016-76492009-090
- 498 Evans, J.A., Tatham, S., 2004. Defining “local signature” in terms of Sr isotope composition using a
499 tenth- to twelfth-century Anglo-Saxon population living on a Jurassic clay-carbonate terrain,
500 Rutland, UK. *Geol. Soc. London, Spec. Publ.* 232, 237–248. doi:10.1144/GSL.SP.2004.232.01.21
- 501 Faure, G., Mensing, T.M., 2005. *Isotopes: Principles and Applications*, 3rd ed. John Wiley and Sons Inc.,
502 Hoboken, New Jersey.
- 503 Frei, K.M., Frei, R., 2011. The geographic distribution of strontium isotopes in Danish surface waters – A
504 base for provenance studies in archaeology, hydrology and agriculture. *Appl. Geochemistry* 26,
505 326–340. doi:10.1016/j.apgeochem.2010.12.006
- 506 Frei, R., Frei, K.M., 2013. The geographic distribution of Sr isotopes from surface waters and soil
507 extracts over the island of Bornholm (Denmark) - A base for provenance studies in archaeology and
508 agriculture. *Appl. Geochemistry* 38, 147–160. doi:10.1016/j.apgeochem.2013.09.007
- 509 Goovaerts, P., 1998. Ordinary Cokriging Revisited 1. *Math. Geol.* 30, 21–42.
510 doi:10.1023/A:1021757104135
- 511 Gryschnko, R., Kuhnle, R., Terytze, K., Breuer, J., Stahr, K., 2005. Research Articles Soil Extraction of
512 Readily Soluble Heavy Metals and As with 1 M NH_4NO_3 -Solution. *J. Soils Sediments* 5, 101–106.
513 doi:10.1065/jss2004.10.119
- 514 Hall, G.E.M., Maclaurin, A.I., Garrett, R.G., 1998. Assessment of the 1 M NH_4NO_3 extraction protocol
515 to identify mobile forms of Cd in soils. *J. Geochemical Explor.* 64, 153–159.
- 516 Hartman, G., Richards, M., 2014. Mapping and defining sources of variability in bioavailable strontium
517 isotope ratios in the Eastern Mediterranean. *Geochim. Cosmochim. Acta* 126, 250–264.

- 518 doi:10.1016/j.gca.2013.11.015
- 519 Hennig, C., 2015. fpc: Flexible Procedures for Clustering. R package version 2.1-10.
- 520 Hobbs, J.A., Yin, Q., Burton, J., Bennett, W.A., 2005. Retrospective determination of natal habitats for an
521 estuarine fish with otolith strontium isotope ratios. *Mar. Freshw. Res.* 56, 655.
522 doi:10.1071/MF04136
- 523 Hodell, D.A., Quinn, R.L., Brenner, M., Kamenov, G., 2004. Spatial variation of strontium isotopes
524 ($^{87}\text{Sr}/^{86}\text{Sr}$) in the Maya region: A tool for tracking ancient human migration. *J. Archaeol. Sci.* 31,
525 585–601. doi:10.1016/j.jas.2003.10.009
- 526 Kelly, S., Heaton, K., Hoogewerff, J., 2005. Tracing the geographical origin of food: The application of
527 multi-element and multi-isotope analysis. *Trends Food Sci. Technol.* 16, 555–567.
528 doi:10.1016/j.tifs.2005.08.008
- 529 Kootker, L.M., van Lanen, R.J., Kars, H., Davies, G.R., 2016. Strontium isoscapes in The Netherlands.
530 Spatial variations in $^{87}\text{Sr}/^{86}\text{Sr}$ as a proxy for palaeomobility. *J. Archaeol. Sci. Reports* 6, 1–13.
531 doi:10.1016/j.jasrep.2016.01.015
- 532 Krige, D.G., 1951. A Statistical Approach to Some Basic Mine Valuation Problems on the
533 Witwatersrand. University of Witwatersrand. doi:10.2307/3006914
- 534 Laffoon, J.E., Davies, G.R., Hoogland, M.L.P., Hofman, C.L., 2012. Spatial variation of biologically
535 available strontium isotopes ($^{87}\text{Sr}/^{86}\text{Sr}$) in an archipelagic setting: a case study from the Caribbean.
536 *J. Archaeol. Sci.* 39, 2371–2384. doi:10.1016/j.jas.2012.02.002
- 537 Maechler, M., Rousseeuw, P., Struyf, A., Hubert, M., Hornik, K., 2015. cluster: Cluster Analysis Basics
538 and Extensions. R package version 2.0.3.
- 539 Maurer, A.F., Galer, S.J.G., Knipper, C., Beierlein, L., Nunn, E. V., Peters, D., Tütken, T., Alt, K.W.,
540 Schöne, B.R., 2012. Bioavailable $^{87}\text{Sr}/^{86}\text{Sr}$ in different environmental samples - Effects of
541 anthropogenic contamination and implications for isoscapes in past migration studies. *Sci. Total*
542 *Environ.* 433, 216–229. doi:10.1016/j.scitotenv.2012.06.046
- 543 Meers, E., Du Laing, G., Unamuno, V., Ruttens, A., Vangronsveld, J., Tack, F.M.G., Verloo, M.G., 2007.
544 Comparison of cadmium extractability from soils by commonly used single extraction protocols.
545 *Geoderma* 141, 247–259. doi:10.1016/j.geoderma.2007.06.002
- 546 Négrel, P., 1999. Geochemical Study of a Granitic Area – The MargerideMountains, France: Chemical
547 Element Behavior and $^{87}\text{Sr}/^{86}\text{Sr}$ Constraints. *Aquat. Geochemistry* 5, 125–165.
548 doi:10.1023/A:1009625412015

- 549 Négrel, P., Deschamps, P., 1996. Natural and anthropogenic budgets of a small watershed in the massif
550 central (France): Chemical and strontium isotopic characterization of water and sediments. *Aquat.*
551 *Geochemistry* 2, 1–27. doi:10.1007/BF00240851
- 552 Négrel, P., Petelet-Giraud, E., Widory, D., 2004. Strontium isotope geochemistry of alluvial groundwater:
553 a tracer for groundwater resources characterisation. *Hydrol. Earth Syst. Sci.* 8, 959–972.
554 doi:10.5194/hess-8-959-2004
- 555 Pestle, W.J., Simonetti, A., Curet, L.A., 2013. $^{87}\text{Sr}/^{86}\text{Sr}$ variability in Puerto Rico: Geological
556 complexity and the study of paleomobility. *J. Archaeol. Sci.* 40, 2561–2569.
557 doi:10.1016/j.jas.2013.01.020
- 558 Poszwa, A., Dambrine, E., Ferry, B., Pollier, B., Loubet, M., 2002. Do deep tree roots provide nutrients to
559 the tropical rainforest? *Biogeochemistry* 60, 97–118. doi:10.1023/A:1016548113624
- 560 Poszwa, A., Ferry, B., Dambrine, E., Pollier, B., Wickman, T., Loubet, M., Bishop, K., 2004. Variations
561 of bioavailable Sr concentration and $^{87}\text{Sr}/^{86}\text{Sr}$ ratio in boreal forest ecosystems: Role of
562 biocycling, mineral weathering and depth of root uptake. *Biogeochemistry* 67, 1–20.
563 doi:10.1023/B:BIOG.0000015162.12857.3e
- 564 Price, T.D., Burton, J.H.H., Bentley, R.A., 2002. The Characterization of Biologically Available
565 Strontium Isotope Ratios for the Study of Prehistoric Migration. *Archaeometry* 44, 117–135.
566 doi:10.1111/1475-4754.00047
- 567 Price, T.D., Knipper, C., Grupe, G., Smrcka, V., 2004. Strontium Isotopes and Prehistoric Human
568 Migration: The Bell Beaker Period in Central Europe. *Eur. J. Archaeol.* 7, 9–40.
569 doi:10.1177/1461957104047992
- 570 Prohaska, T., Wenzel, W.W., Stingeder, G., 2005. ICP-MS-based tracing of metal sources and mobility in
571 a soil depth profile via the isotopic variation of Sr and Pb. *Int. J. Mass Spectrom.* 242, 243–250.
572 doi:10.1016/j.ijms.2004.11.028
- 573 R Core Team, 2017. *R: A language and environment for statistical computing.*
- 574 Rao, C.R.M., Sahuquillo, A., Lopez Sanchez, J.F., 2008. A review of the different methods applied in
575 environmental geochemistry for single and sequential extraction of trace elements in soils and
576 related materials, *Water, Air, and Soil Pollution*. doi:10.1007/s11270-007-9564-0
- 577 Reimann, C., Birke, M., Demetriades, A., Filzmoser, P., O'Connor, P., O'Connor, P., 2014. Chemistry of
578 Europe's Agricultural Soils. Part A: Methodology and Interpretation of the GEMAS Data Set.
- 579 Saby, N., Arrouays, D., Boulonne, L., Jolivet, C., Pochot, A., 2006. Geostatistical assessment of Pb in soil

- 580 around Paris, France. *Sci. Total Environ.* 367, 212–221. doi:10.1016/j.scitotenv.2005.11.028
- 581 Scheib, A.J., Birke, M., Dinelli, E., GEMAS Project Team, 2014. Geochemical evidence of aeolian
582 deposits in European soils. *Boreas* 43, 175–192. doi:10.1111/bor.12029
- 583 Sillen, A., Hall, G., Richardson, S., Armstrong, R., 1998. $^{87}\text{Sr}/^{86}\text{Sr}$ ratios in modern and fossil food-
584 webs of the Sterkfontein Valley: Implications for early hominid habitat preference. *Geochim.*
585 *Cosmochim. Acta* 62, 2463–2473. doi:10.1016/S0016-7037(98)00182-3
- 586 Slovak, N.M., Paytan, A., 2012. *Handbook of Environmental Isotope Geochemistry*, *Handbook of*
587 *Environmental Isotope Geochemistry*. Springer, Berlin, Heidelberg. doi:10.1007/978-3-642-10637-8
- 588 Song, B.-Y., Ryu, J.-S., Shin, H.S., Lee, K.-S., 2014. Determination of the Source of Bioavailable Sr
589 Using $^{87}\text{Sr}/^{86}\text{Sr}$ Tracers: A Case Study of Hot Pepper and Rice. *J. Agric. Food Chem.* 62, 9232–
590 9238. doi:10.1021/jf503498r
- 591 Vitòria, L., Otero, N., Soler, A., Canals, A., 2004. Fertilizer characterization: isotopic data (N, S, O, C,
592 and Sr). *Environ. Sci. Technol.* 38, 3254–3262.
- 593 Voerkelius, S., Lorenz, G.D., Rummel, S., Quélet, C.R., Heiss, G., Baxter, M., Brach-Papa, C., Deters-
594 Itzelsberger, P., Hoelzl, S., Hoogewerff, J., Ponzevera, E., Van Bockstaele, M., Ueckermann, H.,
595 2010. Strontium isotopic signatures of natural mineral waters, the reference to a simple geological
596 map and its potential for authentication of food. *Food Chem.* 118, 933–940.
597 doi:10.1016/j.foodchem.2009.04.125
- 598 West, J.B., Bowen, G.J., Dawson, T.E., Tu, K.P., 2010. Isoscapes: Understanding movement, pattern, and
599 process on earth through isotope mapping, in: West, J.B., Bowen, G.J., Dawson, T.E., Tu, K.P.
600 (Eds.), *Isoscapes: Understanding Movement, Pattern, and Process on Earth Through Isotope*
601 *Mapping*. Springer Netherlands, pp. 1–487. doi:10.1007/978-90-481-3354-3
- 602 Widga, C., Walker, J.D., Boehm, A., 2017. Variability in Bioavailable $^{87}\text{Sr}/^{86}\text{Sr}$ in the North American
603 Midcontinent. *Open Quat.* 3, 4. doi:10.5334/oq.32
- 604 Willmes, M., McMorrow, L., Kinsley, L., Armstrong, R.A., Aubert, M., Eggins, S., Falguères, C.,
605 Maureille, B., Moffat, I., Grün, R., 2014. The IRHUM (Isotopic Reconstruction of Human
606 Migration) database – bioavailable strontium isotope ratios for geochemical fingerprinting in
607 France. *Earth Syst. Sci. Data* 6, 117–122. doi:10.5194/essd-6-117-2014
- 608 Wunder, M.B., 2012. Determining geographic patterns of migration and dispersal using stable isotopes in
609 keratins. *J. Mammal.* 93, 360–367. doi:10.1644/11-MAMM-S-182.1

610

Highlights

- $^{87}\text{Sr}/^{86}\text{Sr}$ ratios provide a robust framework for archaeological provenance studies in France
- 5 isotope groups were identified using cluster analysis
- Kriging using the clusters as covariates produced accurate $^{87}\text{Sr}/^{86}\text{Sr}$ predictions
- This method provides a geologically and sample density informed estimate of spatial uncertainty